Numerical simulation of motion of table tennis ball; Effect of ball diameter

Yutaka TSUJI and Yoshitsugu MUGURUMA
Department of Mechanical Engineering, Osaka University, Japan

1 Introduction

Yuza et al. (1992) showed statistical data on table tennis such as rally time and the number of strokes. We found from their analysis that the number of rallies smaller in table tennis than other racket sports like lawn tennis. Unfortunately, the less the number of rallies, the less attractive table tennis game is for the spectators. To make table tennis a more attractive sport for spectators, the increase in the number of rallies is essential. Some ideas can be considered for that purpose; for instance, change in net height, change in table size and change in ball weight and size. These quantities are specified as rules by the international organization of table tennis and have not changed for many years. People are accustomed to playing it under the present systems. Therefore, we should be careful about the influence of change in rules. Among the above changes, change in ball size and weight is considered to be easiest. The authors studied the effects of ball size on ball motion using computer simulation based on fluid mechanics.

Some people have already made this kind of analysis, for instance, Ushiyama et al. (1996), Seydel (1992), Tiefenbacher & Durey (1994), Durey & Roland (1994), Yamamoto et al. (1996), Tiefenbacher et al. (1996). These reports indicated that it is possible to predict ball motion by using techniques of numerical analysis. Following these studies, the present work was performed to offer the data for people who are interested in the effects of ball size on ball motion.

2 Formulation

2.1 Equation of motion

In general, a table tennis ball has two kinds of motions in the play; translational and rotational motions. These motions are described by the following equations.

$$\ddot{r} = \frac{F}{m} + g \tag{1}$$

$$\dot{\omega} = \frac{T}{I} \tag{2}$$

r : position vector Υ of the ball, m: mass of the ball, ***F***: summation of forces acting on the ball, g: gravity acceleration vector, ω : angular velocity vector of the ball, I: moment of inertia of the ball, $2/3(D_p/2)^2m$, D_p: ball diameter, T: summation of torque, $(\dot{\ })$: time derivative.

The force F consists of fluid forces F_f such as drag and lift except at the moment of collision of the ball against the table. When the ball collides with the table, the contact force F_c is also included in F. In the same sense, the torque T acting on the ball is caused by the fluid viscosity, T_f, while the ball is flying but when the ball collides with the table, the torque T_c due to the contact force should be taken into account.

Therefore in general,

$$F = F_c + F_f \tag{3}$$

$$T = T_c + T_f \tag{4}$$

Expressions of the above forces are given later.

The motion of the ball is obtained by integrating Eqn.(1) and Eqn.(2) numerically, that is, the new velocity and position after the time step Δt are calculated as follows:

$$v = v_0 + \ddot{r}_0 \Delta t \tag{5}$$

$$r = r_0 + v\Delta t \tag{6}$$

$$\omega = \omega_0 + \dot{\omega}_0 \Delta t \tag{7}$$

where v is the velocity vector, subscript 0 denotes the old value. $\ddot{r}_0$ and $\dot{\omega}_0$ are given by Eqn.(1) and Eqn.(2).

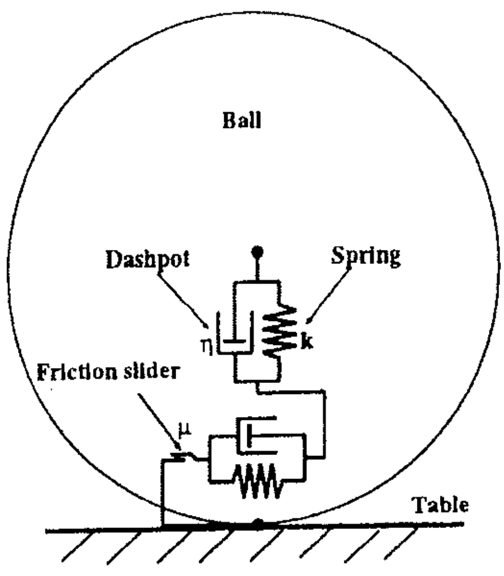

Figure 1. Model of the constant force

2.2 Contact force

The contact forces and are estimated by using the kinetic model (Tsuji et al., 1992) in Figure 1 which was proposed by Cundall and Strack (1979). As shown in Figure 1, modeling is made with the mechanical elements such as spring, dash-pot and friction slider. The following parameters affect the ball motion quantitatively.

Spring constant	k
Damping coefficient	η
Friction coefficient	μ

In this calculation, k is given based on the Hertzian non-linear spring (Tsuji et al., 1992). η is estimated from the coefficient of restitution e (Tsuji et al., 1992). e is determined by a repulsive test of a ball falling on the table. The method of the test is specified officially. The test is made by the following procedure. The ball is at rest initially and the initial position is at 30 cm above the table. The ball is let fall and rebound height is measured. The ball which has rebound height of 23 cm is used for an official instrument. According to a test, the value of is estimated to be 0.88 , and thus this value was used in this work .

2.3 Fluid drag force

The fluid force $\boldsymbol{F}_f$ acting on a flying ball is given,

$$F_f = \frac{1}{2}\rho_f |v| A\left(-C_D v + C_{LR}\frac{-v\times\omega}{|\omega|}\right) \tag{8}$$

where A is sectional area of the ball, ρ_f is the density of the air. The first term of the right hand side means the drag force, the second term is the lift force caused by the rotation of the ball.

The drag coefficient C_D is given by Morsi and Alexander (1972)

$$C_D = C_0 + \frac{C_1}{\mathrm{Re}_p} + \frac{C_2}{\mathrm{Re}_p^{\ 2}} \tag{9}$$

where C_0, C_1, C_2 are constants shown in Table 1. R_{ep} in the table is the ball Reynolds number defined by

$$\mathrm{Re}_p = \frac{|v| D_p \rho_f}{\eta_f} \tag{10}$$

where η_f is viscosity of the air, and D_p is the ball diameter.

The lift coefficient C_{LR} is given by Tsuji (1984)

$$C_{LR} = \min\left[0.5, \quad 0.5\times\frac{D_p|\omega|}{2|v|}\right] \tag{11}$$

The torque T_f on a rotating ball exerted by viscous fluid is given as follows

(Dennis et al., 1980; Takagi, 1977).

$$T_f = -\left(\frac{C_{T1}}{\mathrm{Re}_R^{\ 0.5}} + \frac{C_{T2}}{\mathrm{Re}_R} + C_{T3}\,\mathrm{Re}_R \right) \frac{1}{2} \rho_f \left(\frac{D_p}{2} \right)^5 |\omega|\omega \qquad (12)$$

where C_{T1}, C_{T2}, C_{T3} are constants depending on the rotational Reynolds number, $\mathrm{Re}_R = \dfrac{|\omega| D_p^{\ 2} \rho_f}{4\eta_f}$. Table 2 shows the values of these constants.

Table 1. Constant for drag coefficient C_0, C_1, C_2

R_{ep}	C_0	C_1	C_2
$R_{ep} < 0.1$	0	24.0	0
$0.1 < R_{ep} < 1$	3.69	22.7	0.09
$1 < R_{ep} < 10$	1.22	29.2	-3.89
$10 < R_{ep} < 10^2$	0.617	46.5	-116.7
$10^2 < R_{ep} < 10^3$	0.364	98.3	-2778.0
$10^3 < R_{ep}$	0.357	148.6	-47500.0

Table 2. Constant for drag coefficient C_{T1}, C_{T2}, C_{T3}

R_{eR}	C_{T1}	C_{T2}	C_{T3}
$R_{eR} < 1$	0	$16\ \pi$	0
$1 < R_{eR} < 10$	0	$16\ \pi$	0
$10 < R_{eR} < 20$	5.32	37.2	0.0418
$20 < R_{eR} < 50$	6.44	32.2	0
$50 < R_{eR} < 100$	6.45	32.1	0

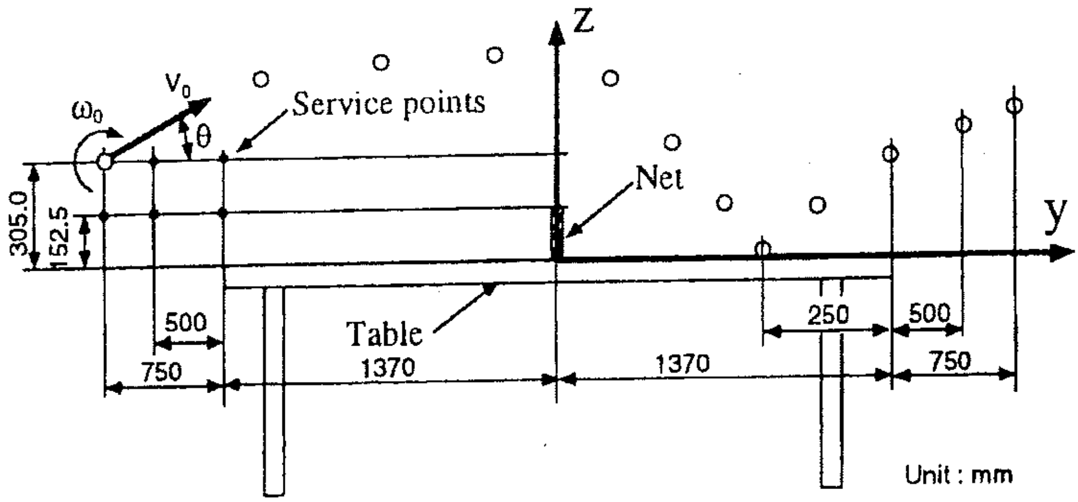

Figure 2. Configuration of the cout

3 Conditions of calculation

Figure 2 shows the schematic diagram of the court. The ball is placed at a service point. The ball is set in motion given the initial velocity v_0, angle θ with horizontal plane and the initial angular velocity ω_0. The direction of rotation is set to make the ball do drive motion.

The conditions in this calculation are shown in Table 3. The initial velocity v_0 and the initial angular velocity ω_0 were decided from the experimental measurement carried out by Ushiyama et al. (1996). The initial velocity v_0 is assumed constant for all the cases in this work. The initial angular velocity ω_0 is changed according to the initial height to send the ball in the opposite court area without netting. In each case of calculation, the angle θ is adjusted so that the ball bounds almost the same point which is 25cm from the end line.

The main purpose of this work is to see the effects of ball diameter on ball motion, and thus cases of three different diameters are considered; 38.0 mm, 39.0 mm and 40.0 mm. The diameter of official balls is 38.0 mm.

Table 3. Common conditions

Mass of ball	2.5 [g]
Initial velocity v_0	46.8[km/h](13[m/s])
Initial angular velocity ω_0	16.7[rps](for initial height 305.0[mm]) 35.0[rps](for initial height 152.5[mm])
Density of air ρ_f	1.205[kg/m^3](at 20 ℃)
Viscisity of air η_f	1.80 $\times 10^{-5}$[Pa·S](at 20 ℃)
Young's modulus of elasticity for the ball	10^6 [Pa]
Coefficient of restitution	0.88
Coefficient of friction	0.3

4 Results and discussion

The results are shown about ball trajectories and velocity variations. The effects of the ball diameter are shown in Figure 3 to Figure 8, where cases of six service points are compared. Tables 5-10 show the data of positions and velocities of the ball at a few selected y-locations. The velocities shown in figures and tables are normalized by the initial value. The selected y-locations are as follows: (1) service point (2) just before bound (3) just after bound (4) end line of the opposite court (5) 500[mm] far from the end line (6) 750[mm] far from the end line. It is found from these figures that the motion of the ball is clearly affected by the increase in diameter by the order of 1 or 2 mm. The larger the diameter, the more the decrease in velocity.

In addition to the study on the effects of ball diameter, other effects such as ball mass, air temperature and altitude were investigated in this work. See Figure 9, Figure 10, Figure 11 and Tables 11-13. These results are obtained based on the standard condition shown in Table 4. The range of change in parameters in these results are not so extreme. However we can observe clearly the effects of the change in these parameters on ball motion which are found to be the same order as in the effects of diameter change. It is interesting that the effects of the altitude are quite remarkable.

Table 4. Standard conditions

Diameter of ball	38.0 [mm]
Mass of ball	2.5 [g]
Density of air ρ_f	1.205[kg/m^3](at 20 ℃)
Viscisity of air η_f	1.80 $\times 10^{-5}$[Pa·S](at 20 ℃)
Service position	y = -2120 [mm], z = 305.0 [mm]

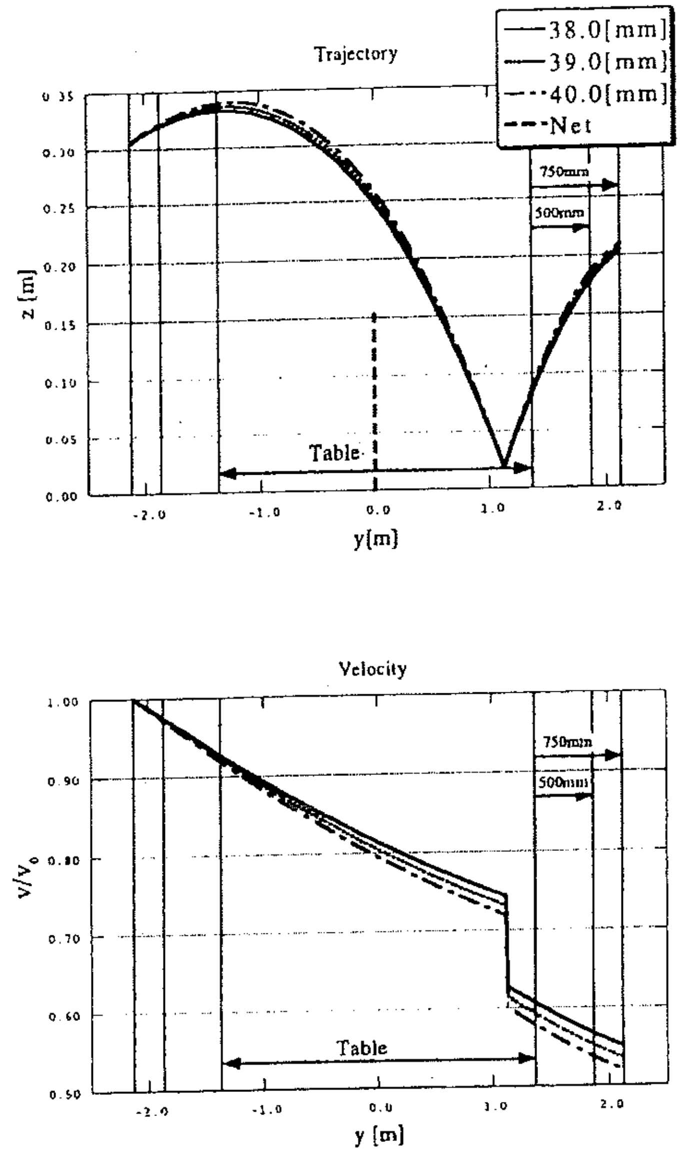

Figure 3. Initial position; z=305mm, y=-2120mm

Table 5. Extract of results

38.0[mm] $\theta = 3.91$[deg]				39.0[mm] $\theta = 4.20$[deg]				40.0[mm] $\theta = 4.51$[deg]				
y[m]	z[m]	V/Vo	W/Wo	y[m]	z[m]	V/Vo	W/Wo	y[m]	z[m]	V/Vo	W/Wo	
-2.120	.3050	1.000	1.000	-2.120	.3050	1.000	1.000	-2.120	.3050	1.000	1.000	initial
1.120	.0189	.744	.989	1.120	.0194	.732	.989	1.120	.0200	.719	.988	befor bound
1.133	.0191	.628	1.439	1.133	.0195	.615	1.439	1.133	.0201	.601	1.438	after bound
1.370	.0834	.606	1.437	1.370	.0862	.593	1.437	1.370	.0885	.579	1.436	opposit side
1.870	.1779	.567	1.433	1.870	.1823	.552	1.432	1.870	.1857	.537	1.431	500mm
2.120	.2032	.551	1.430	2.120	.2069	.535	1.430	2.120	.2092	.520	1.429	750mm

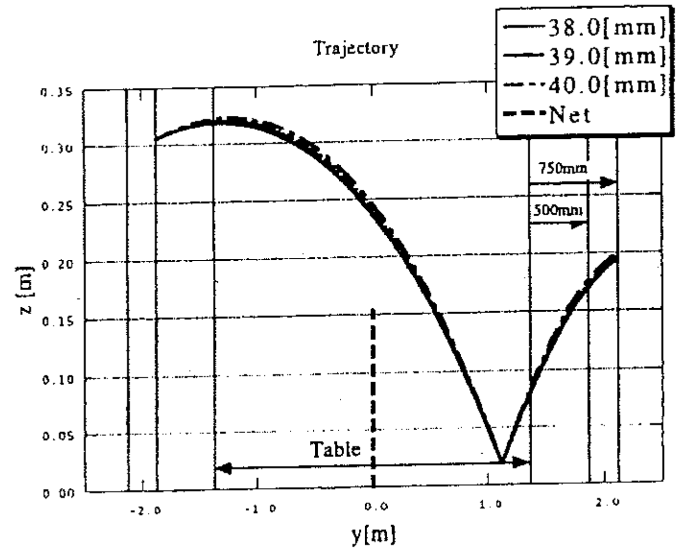

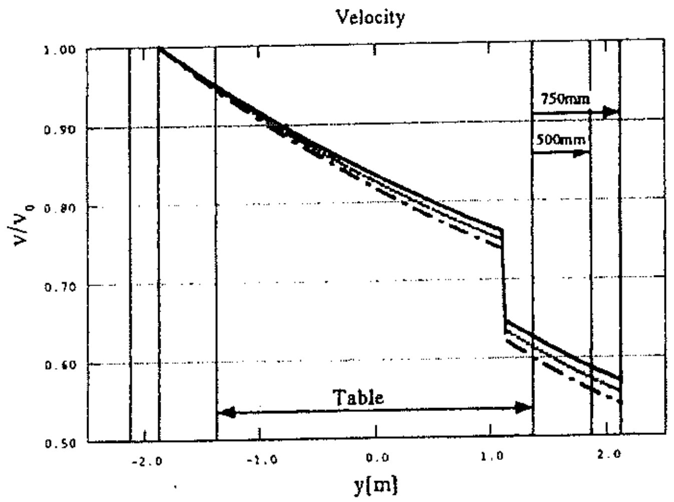

Figure 4. Initial position; z=305mm, y=-1870mm

Table 6. Extract of results

38.0[mm] $\theta = 2.65$[deg]				39.0[mm] $\theta = 2.91$[deg]				40.0[mm] $\theta = 3.18$[deg]				
y[m]	z[m]	V/Vo	W/Wo	y[m]	z[m]	V/Vo	W/Wo	y[m]	z[m]	V/Vo	W/Wo	
-1.870	.3050	1.000	1.000	-1.870	.3050	1.000	1.000	-1.870	.3050	1.000	1.000	initial
1.119	.0189	.761	.990	1.119	.0194	.750	.990	1.119	.0199	.738	.989	befor bound
1.133	.0190	.647	1.436	1.133	.0196	.635	1.436	1.132	.0201	.623	1.436	after bound
1.370	.0803	.626	1.435	1.370	.0820	.613	1.434	1.370	.0847	.600	1.434	opposit side
1.870	.1703	.587	1.431	1.870	.1727	.573	1.429	1.870	.1765	.558	1.429	500mm
2.120	.1947	.570	1.428	2.120	.1960	.556	1.427	2.120	.1991	.541	1.427	750mm

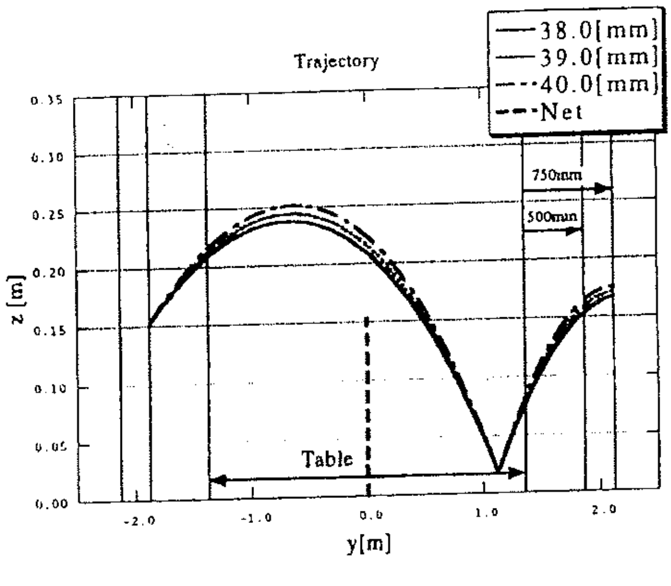

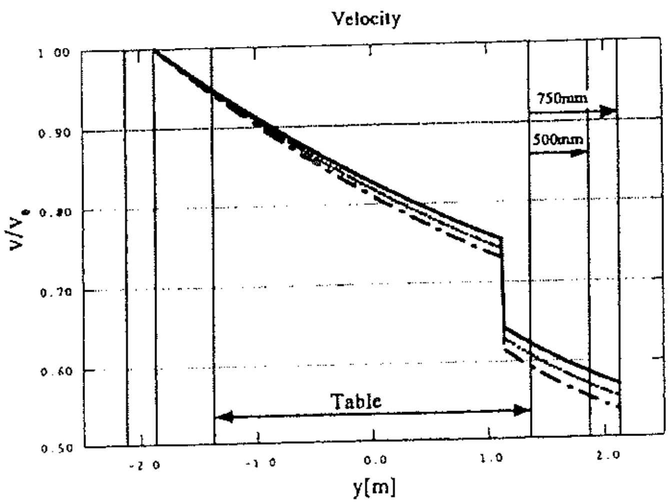

Figure 5. Initial position; z=305mm, y=-1370mm

Table 7. Extract of results

38.0[mm] $\theta = -0.02$[deg]				39.0[mm] $\theta = 0.18$[deg]				40.0[mm] $\theta = 0.39$[deg]				
y[m]	z[m]	V/Vo	W/Wo	y[m]	z[m]	V/Vo	W/Wo	y[m]	z[m]	V/Vo	W/Wo	
-1.370	.3050	1.000	1.000	-1.370	.3050	1.000	1.000	-1.370	.3050	1.000	1.000	initial
1.119	.0190	.798	.992	1.119	.0194	.788	.992	1.119	.0200	.778	.991	befor bound
1.134	.0190	.686	1.435	1.134	.0196	.675	1.434	1.133	.0200	.664	1.433	after bound
1.370	.0752	.665	1.433	1.370	.0768	.653	1.432	1.370	.0786	.642	1.431	opposit side
1.870	.1595	.625	1.429	1.870	.1613	.612	1.428	1.870	.1636	.599	1.427	500mm
2.120	.1831	.607	1.427	2.120	.1841	.594	1.426	2.120	.1854	.581	1.424	750mm

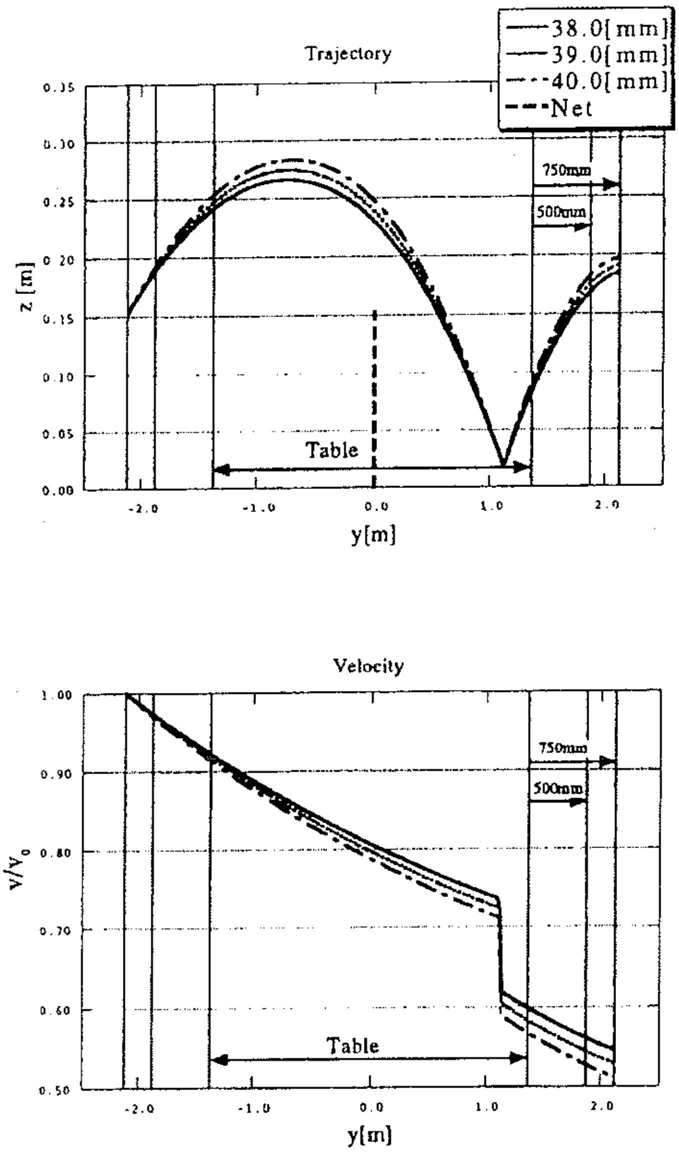

Figure 6. Initial position; z=152.5mm, y=-2120mm

Table 8. Extract of results

38.0[mm] $\theta = 9.07$[deg]				39.0[mm] $\theta = 9.58$[deg]				40.0[mm] $\theta = 10.12$[deg]				
y[m]	z[m]	V/Vo	W/Wo	y[m]	z[m]	V/Vo	W/Wo	y[m]	z[m]	V/Vo	W/Wo	
-2.120	.1525	1.000	1.000	-2.120	.1525	1.000	1.000	-2.120	.1525	1.000	1.000	initial
1.120	.0189	.736	.985	1.120	.0195	.724	.984	1.119	.0200	.712	.983	befor bound
1.133	.0191	.620	1.199	1.133	.0196	.605	1.200	1.132	.0201	.590	1.200	after bound
1.370	.0830	.599	1.197	1.370	.0868	.583	1.198	1.370	.0911	.567	1.198	opposit side
1.870	.1683	.561	1.193	1.870	.1750	.544	1.193	1.870	.1821	.527	1.193	500mm
2.120	.1849	.545	1.190	2.120	.1909	.528	1.190	2.120	.1970	.511	1.190	750mm

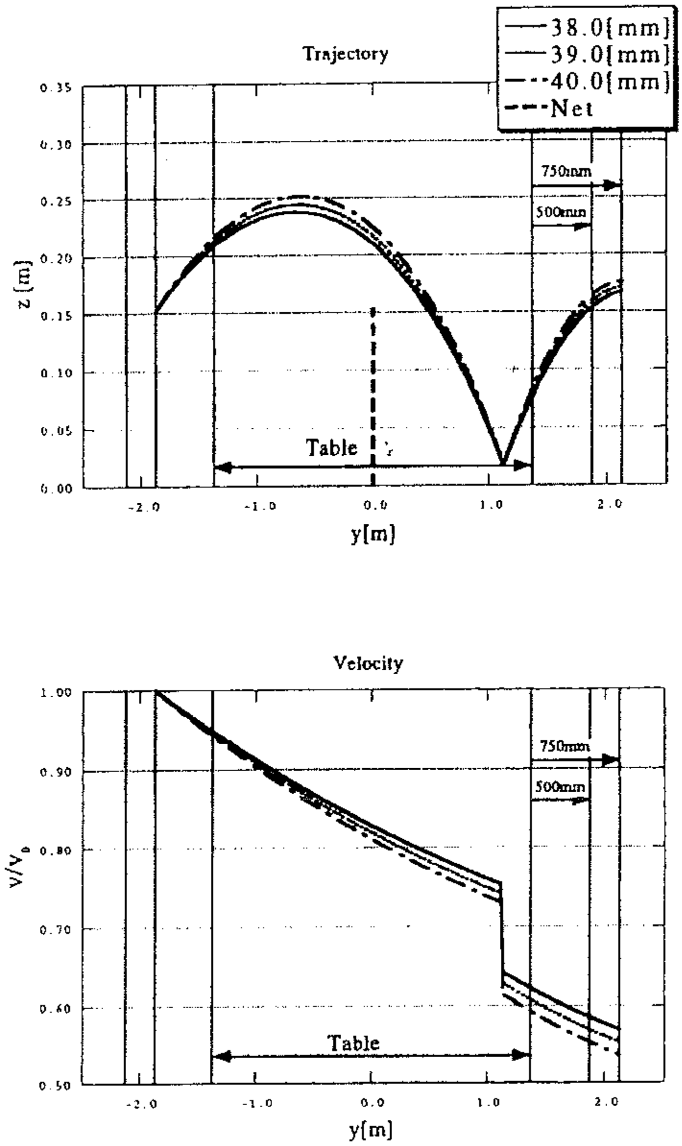

Figure 7. Initial position; z=152.5mm, y=-1870mm

Table 9. Extract of results

38.0[mm] $\theta = 7.81$[deg]				39.0[mm] $\theta = 8.26$[deg]				40.0[mm] $\theta = 8.75$[deg]				
y[m]	z[m]	V/Vo	W/Wo	y[m]	z[m]	V/Vo	W/Wo	y[m]	z[m]	V/Vo	W/Wo	
-1.870	.1525	1.000	1.000	-1.870	.1525	1.000	1.000	-1.870	.1525	1.000	1.000	initial
1.120	.0190	.753	.986	1.119	.0194	.742	.985	1.120	.0200	.730	.985	befor bound
1.134	.0190	.643	1.196	1.132	.0196	.629	1.197	1.133	.0201	.615	1.197	after bound
1.370	.0768	.623	1.194	1.370	.0802	.608	1.195	1.370	.0834	.593	1.195	opposit side
1.870	.1530	.585	1.190	1.870	.1583	.569	1.190	1.870	.1640	.553	1.190	500mm
2.120	.1669	.569	1.188	2.120	.1712	.553	1.187	2.120	.1761	.536	1.187	750mm

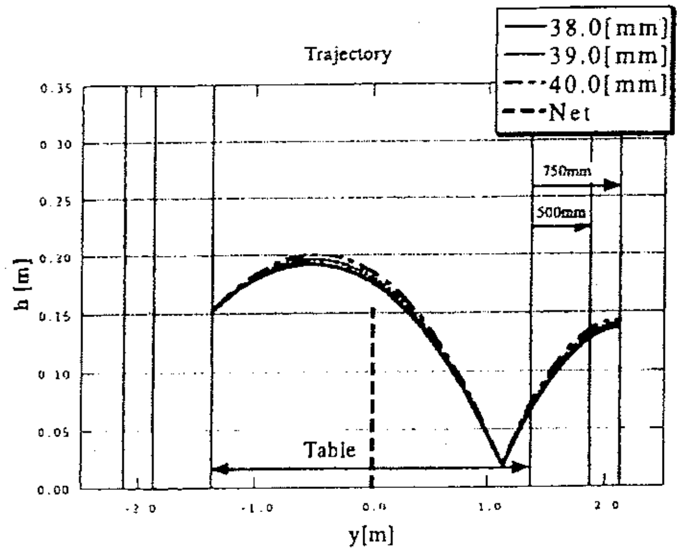

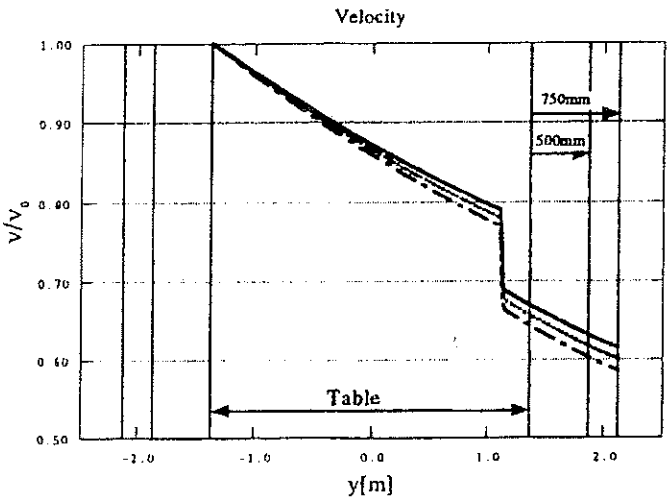

Figure 8. Initial position; z=152.5mm, y=-1370mm

Table 10. Extract of results

38.0[mm] $\theta = 5.29$[deg]				39.0[mm] $\theta = 5.24$[deg]				40.0[mm] $\theta = 6.02$[deg]				
y[m]	z[m]	V/Vo	W/Wo	y[m]	z[m]	V/Vo	W/Wo	y[m]	z[m]	V/Vo	W/Wo	
-1.370	.1525	1.000	1.000	-1.370	.1525	1.000	1.000	-1.370	.1525	1.000	1.000	initial
1.120	.0189	.790	.989	1.119	.0194	.780	.988	1.120	.0199	.770	.988	befor bound
1.136	.0191	.690	1.190	1.134	.0195	.678	1.190	1.134	.0201	.666	1.190	after bound
1.370	.0665	.670	1.188	1.370	.0691	.657	1.188	1.370	.0715	.644	1.188	opposit side
1.870	.1277	.632	1.184	1.870	.1316	.618	1.184	1.870	.1352	.603	1.184	500mm
2.120	.1371	.615	1.182	2.120	.1401	.601	1.182	2.120	.1427	.586	1.181	750mm

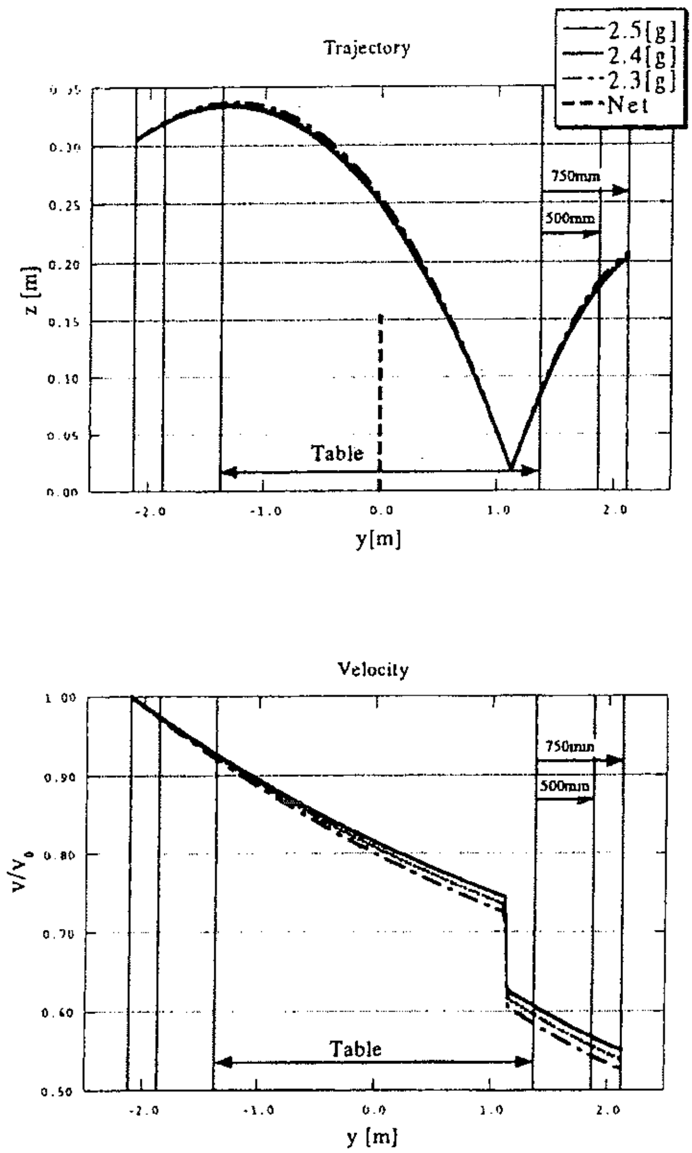

Figure 9. Effect of ball mass

Table 11. Extract of results

2.5[g] $\theta = 3.91$[deg]				2.4[g] $\theta = 4.08$[deg]				2.3[g] $\theta = 4.27$[deg]				
y[m]	z[m]	V/Vo	W/Wo	y[m]	z[m]	V/Vo	W/Wo	y[m]	z[m]	V/Vo	W/Wo	
-2.120	.3050	1.000	1.000	-2.120	.3050	1.000	1.000	-2.120	.3050	1.000	1.000	initial
1.120	.0189	.744	.989	1.119	.0190	.734	.989	1.120	.0189	.724	.988	befor bound
1.133	.0191	.628	1.439	1.133	.0191	.618	1.445	1.132	.0190	.607	1.451	after bound
1.370	.0834	.606	1.437	1.370	.0850	.596	1.443	1.370	.0867	.585	1.449	opposit side
1.870	.1779	.567	1.433	1.870	.1803	.556	1.438	1.870	.1832	.544	1.444	500mm
2.120	.2032	.551	1.430	2.120	.2050	.539	1.436	2.120	.2072	.526	1.442	750mm

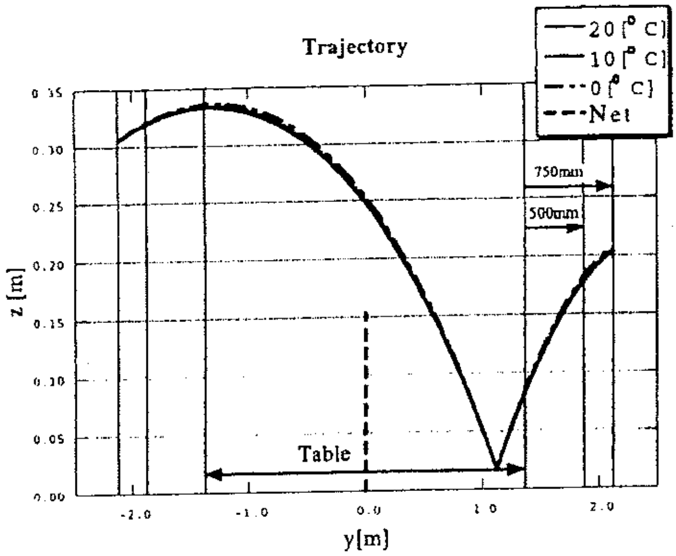

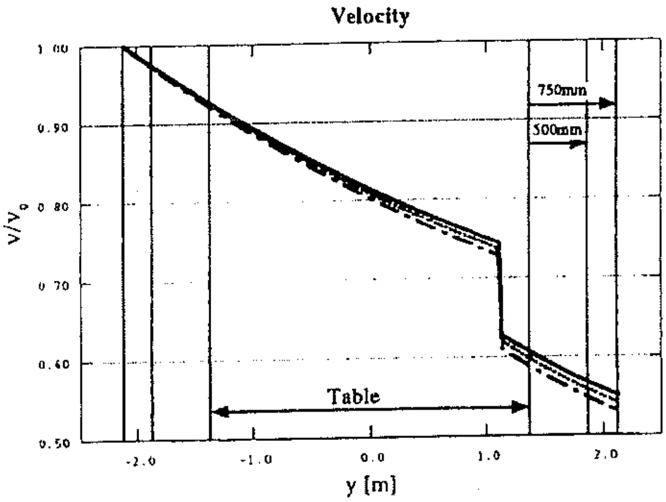

Figure 10. Effect of air temperature

Table 12. Extract of results

20[℃] $\theta = 3.91$[deg] $\rho_f = 1.205$[kg/m^3] $\eta_f = 1.80 \times 10^{-5}$[Pa·S]				10[℃] $\theta = 4.05$[deg] $\rho_f = 1.247$[kg/m^3] $\eta_f = 1.75 \times 10^{-5}$[Pa·S]				0[℃] $\theta = 4.21$[deg] $\rho_f = 1.293$[kg/m^3] $\eta_f = 1.70 \times 10^{-5}$[Pa·S]				
y[m]	z[m]	V/Vo	W/Wo	y[m]	z[m]	V/Vo	W/Wo	y[m]	z[m]	V/Vo	W/Wo	
-2.120	.3050	1.000	1.000	-2.120	.3050	1.000	1.000	-2.120	.3050	1.000	1.000	initial
1.120	.0189	.744	989	1.119	.0190	.736	.989	1.120	.0189	.727	.989	befor bound
1.133	.0191	.628	1.439	1.133	.0191	.620	1.439	1.133	.0190	.611	1.440	after bound
1.370	.0834	.606	1.437	1.370	.0846	.598	1.437	1.370	.0860	.588	1.438	opposit side
1.870	.1779	.567	1.433	1.870	.1798	.558	1.433	1.870	.1824	.548	1.434	500mm
2.120	.2032	.551	1.430	2.120	.2046	.541	1.431	2.120	.2069	.531	1.431	750mm

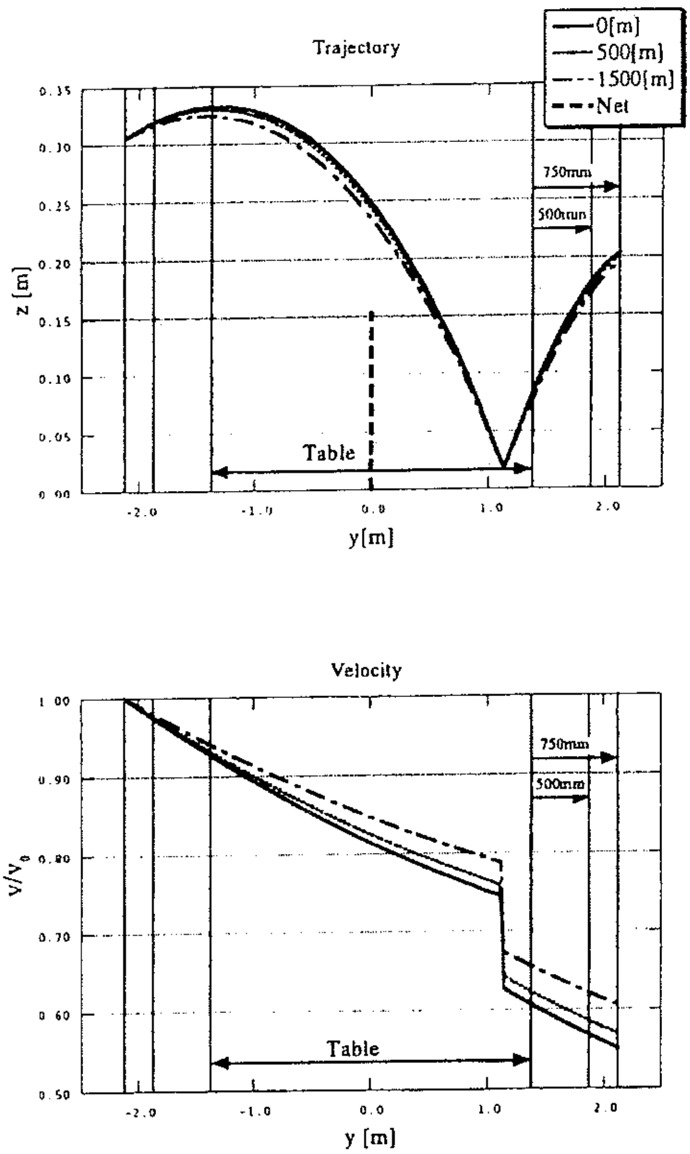

Figure 11. Effect of altitude

Table 13. Extract of results

0[m] $\theta = 3.91$[deg] $\rho_f = 1.205$[kg/m^3]				500[m] $\theta = 3.65$[deg] $\rho_f = 1.128$[kg/m^3]				1500[m] $\theta = 3.16$[deg] $\rho_f = 0.979$[kg/m^3]				
y[m]	z[m]	V/Vo	W/Wo	y[m]	z[m]	V/Vo	W/Wo	y[m]	z[m]	V/Vo	W/Wo	
-2.120	.3050	1.000	1.000	-2.120	.3050	1.000	1.000	-2.120	.3050	1.000	1.000	initial
1.120	.0189	.744	.989	1.119	.0190	.758	.990	1.119	.0190	.788	.991	befor bound
1.133	.0191	.628	1.439	1.133	.0190	.643	1.438	1.133	.0190	.674	1.437	after bound
1.370	.0834	.606	1.437	1.370	.0815	.623	1.436	1.370	.0780	.655	1.435	opposit side
1.870	.1779	.567	1.433	1.870	.1746	.585	1.432	1.870	.1685	.621	1.432	500mm
2.120	.2032	.551	1.430	2.120	.2006	.569	1.430	2.120	.1957	.606	1.430	750mm

5 Concluding remarks

The effects of ball size on ball motion were studied systematically by numerical analysis. The following three sizes were considered; 38.0, 39.0 and 40.0 mm. The increase in ball size leads to the decrease in ball speed. However the judgment of whether the present range of size change will be effective in increasing the number of rally is left to readers of this report.

6 References

Cundall PA and Strack ODL (1979) Geotechnique, 29-147.
Dennis SCR, Singh SN and Ingham D B (1980) J. Fluid Mech 101: 257.
Durey A and Roland S (1994) Int J Table Tennis Sciences No.2: 15.
Morsi SA and Alexander AJ (1972) J Fluid Mech: 55193.
Seydel R (1992) Int J Table Tennis Sciences No.1: 1.
Takagi H (1977) J Phys Soc Japan: 42319.
Tiefenbacher K and Durey A (1994) Int. J Table Tennis Sciences 2.
Tiefenbacher K et al. (1996) Int. J of Table Tennis Sciences 3: 51.
Tsuji Y (1984) "The fundamentals of pneumatic transport", Yokendo (in Japanese).
Tsuji Y, Tanaka T and Ishida T (1992) Powder Technol: 71239.
Ushiyama Y et al. (1996) Report of Table Tennis, Japan Amateur Sports Association (in Japanese).
Yamamoto F et al. (1996) Int. J Table Tennis Sciences 3: 1.
Yuza N et al. (1992) Int J Table Tennis Sciences 1: 79.